Article

Not peer-reviewed version

Synthesis of Molecularly Imprinted Fluorescent Sensor Based on Biomass Derived Carbon Dots from Tomato Stalks for Detection of Tetracycline

Xuejing Wang , Jing Wang , Guanya Ji , Yihua Zhu , Jun Shi , Mengge Zhang , Chengshun Tang , Hongwei Duan , Xiuxiu Dong , Oluwafunmilola Ola , Qian Liu , Qijian Niu *

Posted Date: 4 September 2025

doi: 10.20944/preprints202509.0468.v1

Keywords: tomato straws; carbon dots; tetracycline; molecular imprinted polymers; fluorescence sensor

 doi:10.20944/preprints202509.0468.v1

Article

Synthesis of Molecularly Imprinted Fluorescent Sensor Based on Biomass Derived Carbon Dots from Tomato Stalks for Detection of Tetracycline

Xuejing Wang [1], Jing Wang [1], Guanya Ji [1], Yihua Zhu [1], Jun Shi [1], Mengge Zhang [1], Chengshun Tang [1], Hongwei Duan [2], Xiuxiu Dong [1], Oluwafunmilola Ola [3], Qian Liu [1] and Qijian Niu [1,*]

[1] Key Laboratory of Modern Agricultural Equipment and Technology, School of Agricultural Engineering, Jiangsu University, Zhenjiang, Jiangsu 212013, China

[2] College of Mechanical and Electrical Engineering, ShiHezi University, Shihezi, Xinjiang 832000, China.

[3] Advanced Materials Research Group, University of Nottingham, NG7 2RD, UK

* Correspondence: author: niuqijian@ujs.edu.cn

Highlights

- A novel carbon dots with excellent fluorescence was prepared from agricultural waste tomato straw.
- The fluorescence sensor of CDs@SiO_2-MIPs was constructed via molecularly imprinted SiO_2 confined carbon dots.
- The developed sensor exhibited high selectivity, a wide linear range, and a low detection limit for TC detection.

Abstract

In this work, a novel biomass derived carbon dots (CDs) with superior fluorescent properties were prepared by tomato straws. The selective, eco-friendly sensor for the detection of tetracycline (TC) was developed by grafting SiO_2 molecular imprinted polymers onto the surface of CDs (CDs@SiO_2-MIPs). This sensor combined the high selective adsorption property with the sensitivity of fluorescence detection, which sensing mechanism stems from the off fluorescent signal after the molecular imprinting specifically recognizing the target substance. Under optimal conditions, the fluorescence intensity of the sensor decreased linearly with increasing the concentration of TC from 1.00×10^{-7} to 5.00×10^{-4} mol/L. The detection limit of TC was 9.33×10^{-8} mol/L. This work provides a novel biomass derived CDs and a simple molecularly imprinted fluorescence sensing method for the detection of environmental organic pollutants.

Keywords: tomato straws; carbon dots; tetracycline; molecular imprinted polymers; fluorescence sensor

1. Introduction

Tetracycline antibiotics (TCs), a type of broad-spectrum antibiotics, are widely used in the medical and veterinary fields for the treatment of bacterial infections and as feed additives, due to their low cost and broad-spectrum antibacterial properties[1–3]. However, the excessive and continuous utilization of TC has caused residue in animal-derived foods (e.g. milk, meat, egg products) and pollution of water environment[4]. They enter the human body through bioaccumulation and further lead to a series of adverse effects, including allergic reactions, hepatotoxicity and gastrointestinal disturbance[5]. Currently, traditional methods including high-performance liquid chromatography (LC−ESI-MS−MS)[6], liquid chromatography-mass spectrometry (LC-MS)[7], and enzyme-linked immunosorbent assay (ELISA)[8] are widely employed

 doi:10.20944/preprints202509.0468.v1

for the detection of TC residues. However, in recent years, more cost-effective, convenient, and rapid detection methods compared to traditional approaches have been developed, including electrochemical, photoelectrochemical, colorimetric and fluorescence methods. Among them, fluorescence method has emerged as a promising approach in the field of analysis due to its advantages of high sensitivity, good accuracy, fast response speed and low cost.

It is reported that there are various fluorescent materials that can be used to detect TC, including quantum dots[9–11], nanoclusters[12,13], metal-organic frameworks (MOFs)[14–17], covalent organic frameworks (COFs)[18,19]. Among them, carbon dots (CDs), as a new type of luminescent nanomaterials, have attracted much attention because of their superior fluorescence characteristic, good solubility and hypotoxicity[20]. In 2014, Yan et al.[21] proposed a green preparative strategy of CDs by using biomass small molecule-citric acid as carbon precursors for the first time. Biomass, as a natural, abundant and renewable carbon resource, has been widely used as a carbon source for the preparation of CDs due to the advantages of high carbon content, aromatic structure in components, which is conducive to the formation of conjugated carbon cores (sp^2/sp^3 hybridized), and the presence of heteroatoms such as N, S and P, as well as rich functional groups such as -OH, -COOH and -NH_2[22]. So far, a lot of biomass has been used to prepare carbon-based TC fluorescence sensors, such as rice residue[23], R. graveolens leaves[24], green jujube[25], passion fruit peels[26], Curcuma amada[27], Ophiopogon japonicus f. nanus[28]. All these works have achieved good analytical performance. Nevertheless, the methodology for the TC detection using CDs derived from tomato stalks remains to be investigated. Tomato stalks were ranked as the fourth largest agricultural wastes after the three major crop residues of rice, wheat and corn[29] These vegetable residues are inappropriate for silage, due to the relatively high levels of pesticide and herbicide residues[30,31]. As a result, these vegetable crop residues are either disposed of in landfills or burned on site, which has caused severe environmental pollution and waste of resources[32]. Therefore, the construction of TC fluorescence sensors based on CDs derived from tomato straw not only effectively solves the problem of resource utilization of tomato straw waste in facilities, but also realizes the effective detection of agricultural environmental pollutants, which has dual significance. However, the selectivity of fluorescence sensors based on pure biomass CDs needs to be improved. The molecularly imprinted polymers (MIPs) developed based on the antigen-antibody principle has shown great potential as recognition units in sensing platforms, and it has become an ideal choice for improving the selectivity of fluorescence detection[33–37]. It has the advantages of good physical and chemical stability, simple preparation, low cost[38], and can also withstand high temperatures, high pressures, acids, alkalis and organic solvents[39]. Therefore, molecular imprinting technology is a simple and low-cost option for improving the selectivity of TC fluorescence detection.

In this research, an eco-friendly CDs were synthesized from tomato stalks and subsequently encapsulated into SiO_2-MIPs via a sol-gel approach. The fluorescence of CDs@SiO_2-MIPs sensor exhibited concentration-dependent quenching upon interaction with TC molecule, which was attributed to the inner filter effect (IEF) and static quenching mechanism between TC and CDs@SiO_2-MIPs (Scheme 1). The experimental results demonstrated that the CDs@SiO_2-MIPs sensor exhibited high selectivity, a wide linear range, and a low detection limit for TC. This work adopted a green, economical and facile strategy for synthesizing CDs from renewable plant resources and explored their application in TC detection, which not only holding significance for investigating natural product derived CDs, but also offers novel perspectives for TC monitoring.

 doi:10.20944/preprints202509.0468.v1

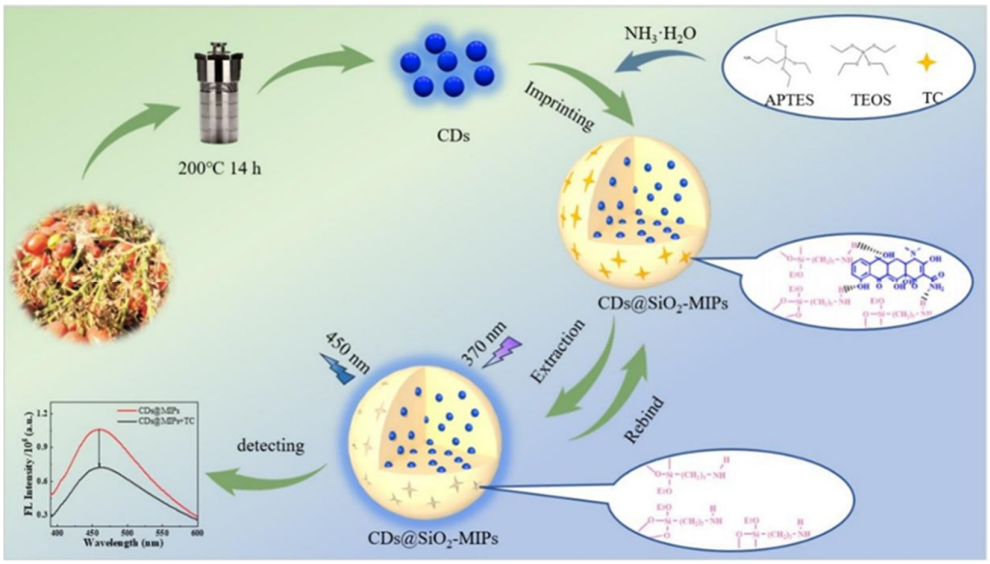

Scheme 1. Schematic illustration of the preparation and detection process of CDs@SiO2-MIPs.

2. Materials and Methods

2.1. Materials

Tetracycline (TC), chlortetracycline (CTC) and sulfamethazine (SDM) were gained from Macklin Biochemical Co., Ltd. (Shanghai, China). Oxytetracycline (OTC) and enrofloxacin (ENR) were obtained from InnoChem Science & Technology Co., Ltd. (Beijing, China). TEOS (tetraethoxysilane), APTES (3-aminopropyl-triethoxy-silane), were purchased from Sigma-Aldrich Trading Co., Ltd (Shanghai, China). Ammonia solution (25% in water), acetic acid, methanol, and ethanol were bought from Sinopharm Chemical Reagent Co., Ltd. (Shanghai, China). All reagents were of analytical grade, and used without further purification. Millipore Milli-Q ultrapure water (18.2 MΩ cm) was used throughout the whole research.

2.2. Apparatus

Transmission electron microscopy (TEM) images were conducted on a Hitachi HT7800 high contrast transmission electron microscope (Hitachi, Japan). Scanning electron microscopy (SEM) was performed using a Hitachi Regulus-8100 field emission scanning electron microscope (Hitachi, Japan). X-ray diffraction (XRD) was acquired using a Bruker-D8 advance (Bruker, Germany). X-ray photoelectron spectroscopy (XPS) was performed using an AXIS SUPRA (Shimadzu, Japan). Ultraviolet-visible (UV-vis) spectra were measured by a UV-3600 plus ultraviolet-visible spectrophotometer (Shimadzu, Japan). FL spectra and FL lifetime were measured on an FS5 FL spectrophotometer (Edinburgh Instruments, UK).

2.3. Preparation of CDs

In a typical experiment, CDs were prepared according to the previously reported method with a little modification[40]. Briefly, Fresh tomato stalks were collected from the Greenhouse located in Jiangsu University. First, tomato stalks were washed using tap water followed by distilled water, and then dried in an incubator at 60°C for 12 h. Dried straws were crushed manually into powder. Then, 1.5 g powder of tomatoes stalk was dispersed in 30 mL of ultrapure water. It was moved into a 50 mL Teflon-lined autoclave after sonication for 20 min and heated in an oven at 200°C for 14 h. After the samples were naturally cooled to room temperature, they were centrifuged and filtered to obtain a dark brown solution, which was stored in a refrigerator at 4°C.

 doi:10.20944/preprints202509.0468.v1

2.4. Preparation of CDs@SiO_2-MIPs

Briefly, 2 mL of CDs solution and 10 mL of ethanol were added into a flask. Then 80 μL of APTES were added and stirred for 2 h under vigorous stirring to allow the APTES to self-assemble onto the CDs. Template TC (10 mg) was then dissolved in ultrapure water (10 mL) and added to the above solution. After stirring for 15 min, 100 μL of ammonia hydroxide solution (25%) was added, then 100 μL of TEOS and 10 mL of ethanol were added drop by drop. The reaction mixture was stirred at room temperature for 20 h. The final products CDs@SiO_2-MIPs were collected by centrifugation, then washed thoroughly with methanol/acetic acid (95:5, v/v). After each washing step, the supernatant was measured by UV to check whether there was TC residue in the solution. Typically, the CDs@SiO_2-MIPs were washed three times in order to completely remove the TC template. Non-imprinted particles (CDs@SiO_2-NIPs) as a control were prepared similarly, except that the template TC was not added.

2.5. Fluorescent Sensing of TC

The obtained oven dried powder of CDs@SiO_2-MIPs (50 mg) was ultrasonically dispersed in ultrapure water (10 mL) to obtain the fluorescent suspension (5 mg/mL). Then, the suspension (500 μL) and the TC standard solution (500 μL, different concentrations) were mixed. The above solution (800 μL) was transferred to the cuvette, and fluorescence measurements were performed at an excitation wavelength of 370 nm, with the fluorescence spectrum recorded over the range of 380–600 nm. Fluorescence emission at 450 nm was used as the fluorescence analysis signal. Each experiment was repeated three times to carry out.

3. Results and Discussion

3.1. Characterization of CDs

The morphology and particle size of biomass derived CDs were characterized by TEM (Figure 1A). The CDs were spherical and relatively monodisperse, with average diameters of approximately 14.20 nm[40].To evaluate the optical properties of the prepared CDs, UV–vis absorption spectrum and fluorescence spectrum were carried out. From Figure 1B it can be seen that CDs have a strong absorption at 200 nm and a weak absorption at 280 nm. The fluorescence spectra of CDs with excitation wavelengths between 370 and 470 nm was shown in Figure 1C. The results show that their emission spectra were highly dependent on the excitation wavelength and the fluorescence intensity of CDs reaches the maximum at the excitation wavelength of 430 nm and the emission wavelength of 500 nm. When the excitation wavelength is greater than 430 nm, the emission wavelength of CDs red shifts and the fluorescence intensity also decreases. As one of the most important parameters for evaluating fluorescent material, quantum yield (QY) was measured with FS5 FL spectrophotometer (Figure 1D). The quantum yield of the prepared CDs was 14.7%. It is a relatively high QY in CDs directly prepared from biomass[41–43].

 doi:10.20944/preprints202509.0468.v1

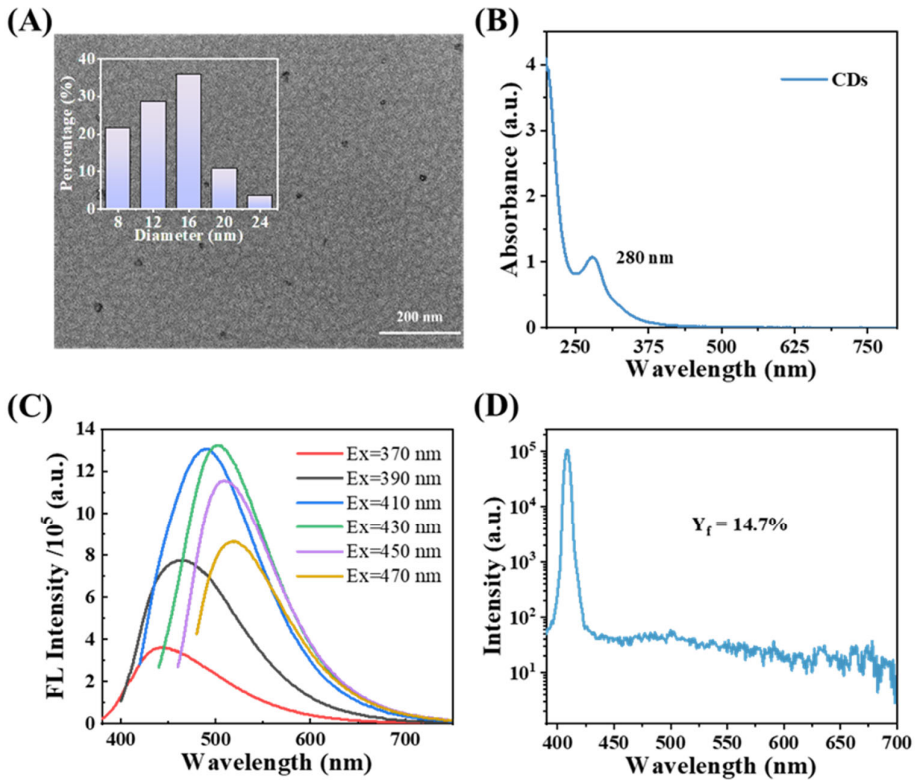

Figure 1. (A) TEM images of CDs; (B) UV–vis absorption spectra of CDs; (C) fluorescence spectra of CDs (excitation wavelength from 370 nm to 470 nm); (D) The FL quantum yield of CDs.

3.2. Characterization of CDs@SiO₂-MIPs

The morphologies of CDs@SiO₂-MIPs were investigated by TEM and SEM, and the particle size was measured by Nano Measurer software, and the particle size distribution was plotted. As shown in Figure 2A, Figure 2B and Figure 2C, the synthesized CDs@SiO₂-MIPs were in regular spherical particle with an average particle size of approximately 0.83 μm. The size of CDs@SiO₂-MIPs is significantly larger than that of CDs, and the imprinting layer of a single CDs@SiO₂-MIPs nanoparticle exhibited a rough morphology (Figure 2B), indicating that CDs have been completely encapsulated by the molecular imprinting layer. The synchronous fluorescence spectra (at 450 nm) of CDs@SiO₂-MIPs before and after the removal of templates were recorded. Figure 2D showed that the synchronous fluorescence intensity of CDs@SiO₂-MIPs was 42.56% of the CDs@SiO₂-NIPs before the removal of TC, but the intensity almost recovered (93.20%) after removal. The result indicated that most of the TC molecules in the specific cavities of CDs@SiO₂-MIPs could be washed out. Meanwhile, the fluorescence intensity of MIPs (spectrum b) is lower than that of NIPs (spectrum a), which is mainly caused by two parts: one is that the MIPs partially lose the luminescent signal of the CDs due to the formation of a relatively thick molecularly imprinted layer composed of functional monomers, as well as the combined effects of APTES, TC, and TEOS. In contrast, the NIPs do not form an imprinted layer due to the absence of polymerization of template molecules with the functional monomers, resulting in a stronger fluorescence signal compared to the MIPs. The second one is that the specific recognition between the alkylamines and carbonyl groups on the exposed quantum dots within the cavities induces non-radiative recombination of electrons, leading to a decrease in fluorescence intensity[44]. Moreover, it can be seen that a symmetric fluorescence emission peak at 450 nm was obtained when excited at 370 nm, which was similar to the CDs characterized above. This indicates that the SiO_2 coating at the surface of CDs does not restrict the photoluminescence properties of CDs[45].

 doi:10.20944/preprints202509.0468.v1

FT-IR spectra of CDs and CDs@SiO_2-MIPs were collected and compared (Figure 2E). The most characteristic peaks of CDs are the absorption bands at 2949 cm^{-1} corresponds to the stretching vibration of the −C−H single bond, the broad adsorption of −OH groups between 3000 cm^{-1} and 3500 cm^{-1}, the band at 1578 cm^{-1} indicates the bending vibration of −N−H, the band at 1351 cm^{-1} corresponds to the −COOH, and the band at 1093 cm^{-1} is related to the stretching vibration of −C−N. As shown in the FT-IR absorption spectrum of CDs@SiO_2-MIPs, the strong and broad peaks around 956 cm^{-1} and 1033 cm^{-1} are assigned to the Si–O–C and Si–O–Si asymmetric stretching, respectively, which is not found in the spectrum of CDs. Peaks at about 778 cm^{-1} and 435 cm^{-1} also suggest the existence of the Si–O vibrations, which indicates that TEOS participated in the synthesis process and displayed a strong cross-linking ability. All the above bands further confirm that the imprinted polymers, generated from sol–gel condensation of APTES and TEOS, have been successfully grafted on the surface of CDs. In addition, the molecular imprinting process leads to no loss of the major functional groups of CDs and has no influence on the subsequent detection.

The XRD pattern of CDs@SiO_2-MIPs was shown in Figure 2F. The broad peak of CDs@SiO_2-MIPs centered at $2\theta = 24°$ can correspond to the C (002) plane. The XRD peak showed the amorphous nature of CDs@SiO_2-MIPs.

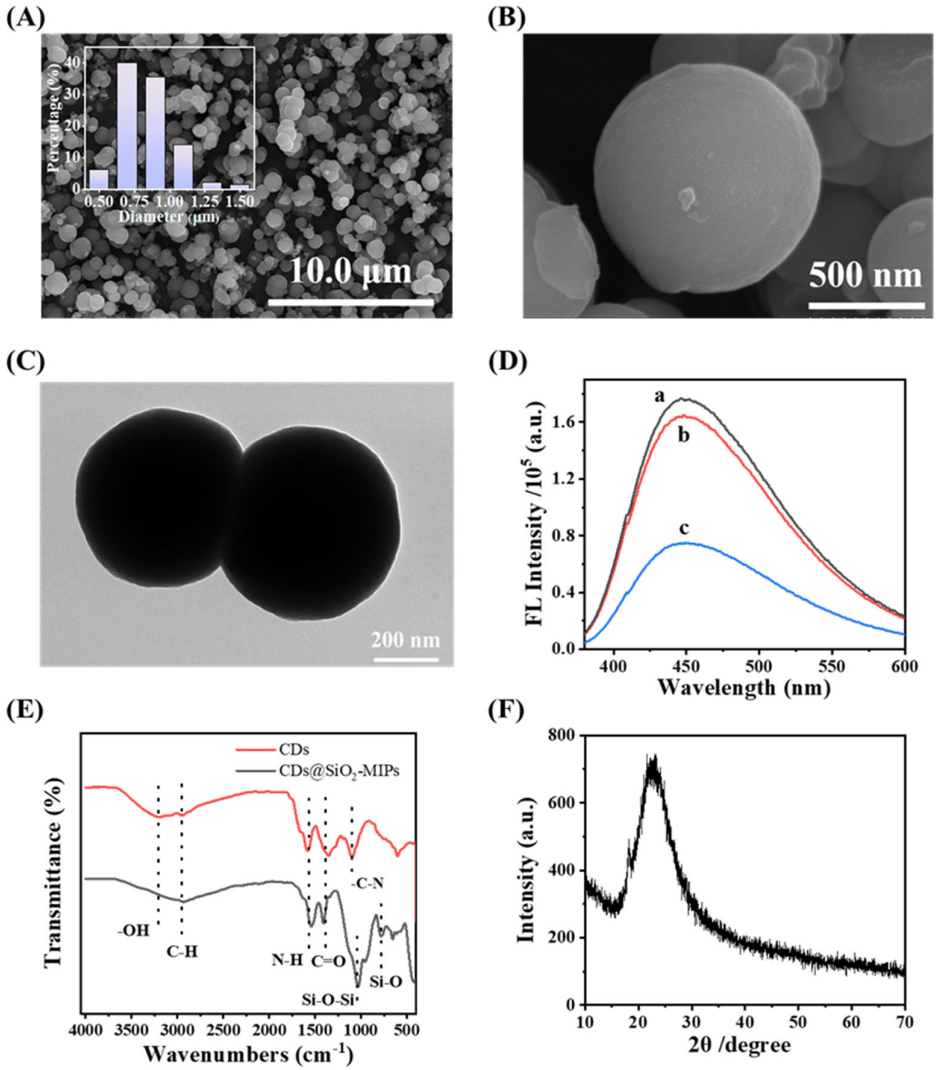

Figure 2. (A), (B) SEM and (C) TEM images of CDs@SiO_2-MIPs; (D) Fluorescence spectra of CDs@SiO_2-NIPs (spectrum a) and CDs@SiO_2-MIPs after (spectrum b) and before (spectrum c) the removal of TC; (E) FT-IR spectra of CDs, CDs@SiO_2-MIPs; (F) XRD pattern of CDs@SiO_2-MIPs.

 doi:10.20944/preprints202509.0468.v1

The elemental composition, contents and chemical bonds of the CDs@SiO_2-MIPs were characterized by XPS. In Figure 3A, the XPS survey spectrum shows four noticeable peaks with the binding energies of 285.2, 400.1, 531.8, and 102.9 eV that correspond to the C 1s, N 1s, O 1s, and Si 2p signals, respectively. The high-resolution spectrum of C 1s in Figure 3B exhibits three peaks at 284.8, 286.1, and 288.3 eV which are assigned to C═C/C–C, C–N, and C═O, respectively. Despite the two peaks of O 1s (Figure 3C) at 531.4 and 532.3 eV ascribed to the existence of C═O and C–OH. Furthermore, as shown in Figure 3D, two peaks exist in the N 1s spectrum at 401.2 and 399.3 eV which are attributed to N–H and C–N bonds, respectively. This information was in accordance with the FT-IR results, and it further confirms that the CDs@SiO_2-MIPs were generated successfully.

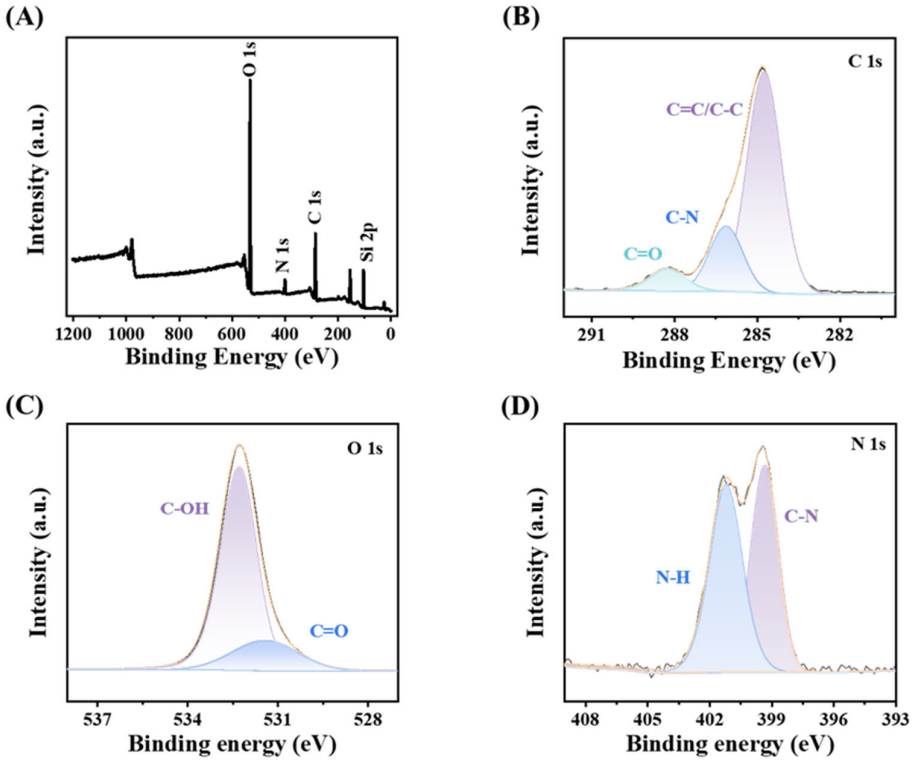

Figure 3. (A) XPS survey scan spectrum; The high-resolution spectrum of C 1s (B); O 1s (C); N 1s (D).

3.3. Optimization of the Sensor

To ensure that the measurements were carried out under ideal conditions, the most important factors impacting the sensor performance were optimized. We investigated the proportion of CDs and functional monomer (APTES) in the fluorescent sensing system to identify the maximum fluorescent intensity. In Figure 4A, the optimal ratio of CDs to functional monomer (APTES) was 50:2, when fluorescence intensity is maximum. After molecularly imprinted polymerization, the effective elution of the fixed template molecules not only facilitates the formation of specific binding cavities and recognition sites, but also prevents the leakage of template molecules during the re-binding process, which could lead to false-positive results. Therefore, the effects of different elution times on the elution efficiency of CDs@SiO_2-MIPs were compared. As shown in Figure 4B, the fluorescence quenching efficiency reached its optimum at an elution time of 30 min. The decrease in quenching efficiency with prolonged time may be attributed to the degradation of imprinted cavities. Therefore, 30 min was selected as the optimal elution duration. The effect of incubation time was also investigated, Figure 4C shows that the fluorescence quenching efficiency of TC towards CDs@SiO_2-MIPs increased rapidly within 0–20 min and remained constant after 20 min, confirming that the binding between TC and the imprinted cavities of CDs@SiO_2-MIPs attained an equilibrium state in 20 min. To ensure effective binding of the imprinted cavities with TC, 25 min was selected as the

 doi:10.20944/preprints202509.0468.v1

optimal incubation time. An excessive amount of CDs@SiO_2-MIPs would result in reduced sensitivity to TC while an insufficient amount may lead to the narrow linear range. Therefore, the amount of CDs@SiO_2-MIPs was optimized. As shown in Figure 4D, the fluorescence quenching efficiency could reach the highest value at the amount of 2.5 mg/mL. The fluorescence quenching efficiency decreased with decreasing the amounts of CDs@SiO_2-MIPs while overmuch CDs@SiO_2-MIPs (2.5 mg/mL) could lead to the self-quenching of fluorescence. Therefore, 2.5 mg/mL of CDs@SiO_2-MIPs was selected as the optimal concentration.

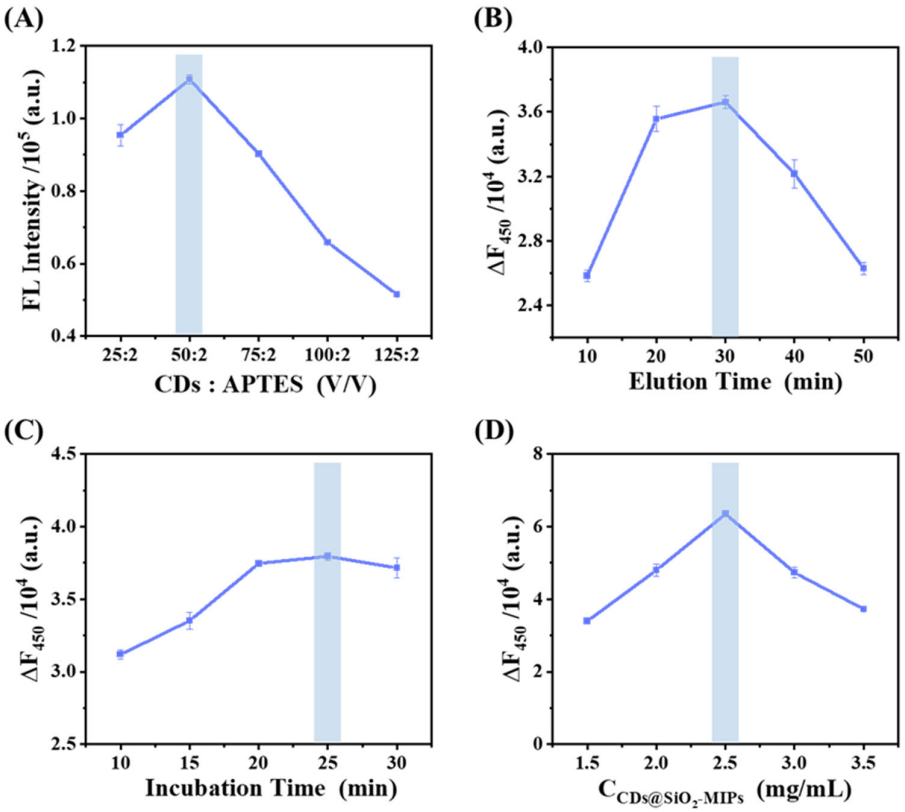

Figure 4. (A) FL Intensity of CDs and APTES at different volume ratios; Effect of (B) elution time; (C) incubation time; (D) CDs@SiO_2-MIPs concentration on CDs@SiO_2-MIPs detection performance.

3.4. Fluorescence Detection of CDs@SiO_2-MIPs Toward TC

Under the optimal conditions, the fluorescence signal of CDs@SiO_2-MIPs sensor at 450 nm decreased with increasing concentrations of TC (Figure 5), which was linearly related to the logarithm of TC concentration, corresponding to the equation $y=-0.33\lg CTC-0.64$ ($R^2=0.995$) (1×10^{-7} ~ 5×10^{-4} mol/L). Furthermore, the limit of detection (LOD) for CDs@SiO_2-MIPs was also expected by using $3\sigma/K$ algorithm formula, in which σ was the blank standard deviation (n = 10) and K was the slope of the algorithm formula. Thus, the LOD for CDs@SiO_2-MIPs was 9.33×10^{-8} mol/L. Overall, the system offered outstanding sensitivity and a wide linear range.

 doi:10.20944/preprints202509.0468.v1

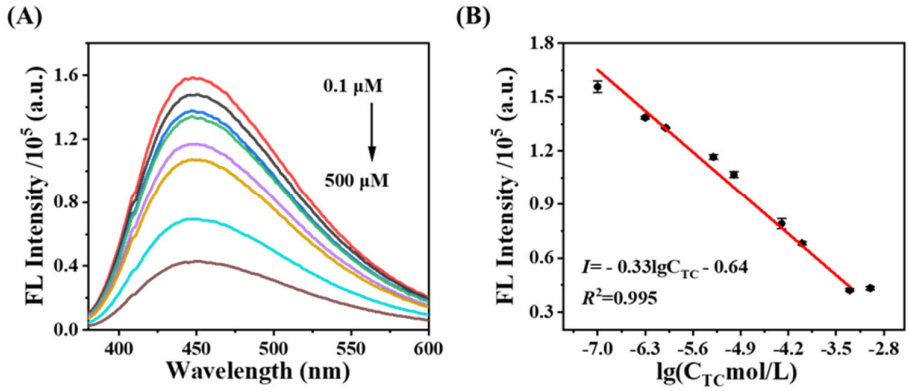

Figure 5. (A) Fluorescence responses of the CDs@SiO_2-MIPs toward different concentrations of TC; (B) Linear relationship between the logarithm of TC concentration and the fluorescence intensity (F_{450}) of CDs@SiO_2- MIPs.

3.5. Mechanism of CDs@SiO_2-MIPs for the TC Detection

For exploring the sensing mechanism of quenching effect occurred in this work, a series of experiments were conducted. Figure 6A depicts the UV absorption peaks of TC, CDs@SiO_2-MIPs and CDs@SiO_2-MIPs with TC. The UV absorption peaks of TC are located at 276 nm and 357 nm, while CDs@SiO_2-MIPs exhibit no significant absorption peaks. However, after mixing CDs@SiO_2-MIPs with TC, the absorption peak of TC originally at 276 nm red-shifted to 282 nm. It indicated that the CDs@SiO_2-MIPs nanoparticles have an interaction with TC to form the ground state complex. The result indicated that the binding of CDs@SiO_2-MIPs with TC was attributed to static quenching.

In addition, as shown in Figure 6B, TC has two obvious ultraviolet absorption peaks, and a good spectral overlap was observed between the ultraviolet absorption peak at 357 nm and the excitation spectrum of CDs@SiO_2-MIPs. This confirms the possibility of the following mechanisms: the inner filter effect (IFE) or/and Förster resonance energy transfer (FRET). IFE is an apparent quenching in which a second absorber filters the emission, resulting in an attenuation of the excited beam[46], whereas FRET is a phenomenon of energy transfer between the excited state of the CDs@SiO_2-MIPs and the ground state of the quencher[34]. The fluorescence lifetime of the CDs@SiO_2-MIPs -quencher system will decrease or increase with FRET, whereas it remains the same or nearly unchanged with IFE[47]. The fluorescence internal filtration effect led to fluorescence quenching of the system by measuring the fluorescence lifetime changes of CDs@SiO_2-MIPs before and after the addition of TC[27]. The effect of TC on the fluorescence lifetime of the sensor was further determined (Figure 6C and Figure 6D), and the results showed that the fluorescence lifetime before and after adsorption of TC respectively was 5.73 ns and 5.61 ns, demonstrated that fluorescence quenching is caused by the IFE mechanism. When the excitation light was irradiated, the continuously adsorbed and accumulated TC on the CDs@SiO_2-MIPs surface absorbed part of the excitation light, resulting in a decrease in the incident light absorbed by the CDs and a significant decrease in the fluorescence of the system.

 doi:10.20944/preprints202509.0468.v1

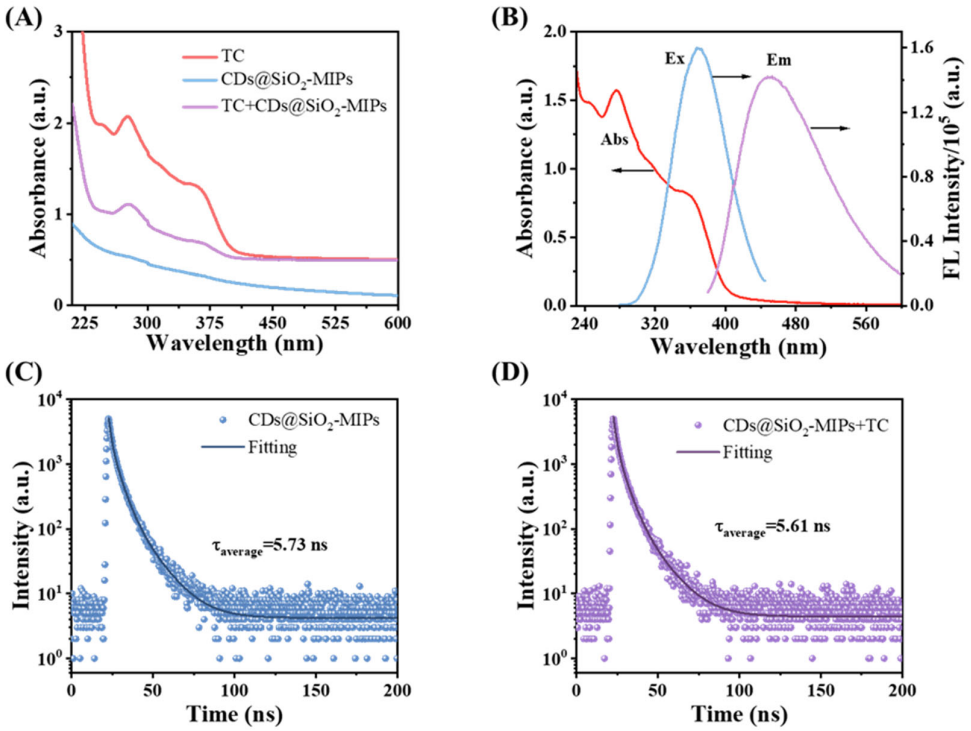

Figure 6. (A) UV–vis spectra of TC, CDs@SiO2-MIPs nanocomposite with TC, CDs, and CDs@SiO2-MIPs nanocomposite; (B) excitation and emission spectra of CDs@SiO2-MIPs and UV–vis absorption spectra of TC; Fluorescence decay profile of the CDs@SiO2-MIPs in the absence (C) and presence (D) of TC.

3.6. Selectivity, Anti-Interference Ability and Stability of CDs@SiO2-MIPs Sensor

The sensing system was further evaluated on the basis of selectivity, anti-interference ability and stability. The selectivity was studied by comparing the fluorescence response to TC, other antibiotics and potential interfering ions, including OTC, CTC, ENR, SDM, K^+, Ca^{2+}, Mg^{2+}, Cu^{2+}, Zn^{2+}, Hg^+, $Cl^-$and SO_4^{2-} (Figure 7A and B). In the presence of 250 μM other antibiotics or ions, the fluorescence intensity at F_{450} remained practically unchanged, whereas the system exhibited an apparent fluorescence response in the presence of 25 μM TC. Although the structures of OTC and CTC were similar to TC, the corresponding changes of fluorescence response were only marginal even at a 10-fold higher concentration compared to TC. This illustrates that the proposed sensing system was extremely selective for TC. Moreover, the fluorescence intensity remained constant when the interferents were added to the system together with TC, confirming that the designed sensing system possessed excellent anti-interference ability.

Optical stability is a critical property of fluorescence sensors. In Figure S1, both CDs and CDs@SiO2-MIPs exhibited minimal fluorescence intensity variations when exposed to 365 nm UV irradiation, demonstrating relative standard deviations (RSDs) of merely 0.63% and 0.94% over 120 min, respectively[48]. These results confirm the remarkable photobleaching resistance of the developed sensor.

Furthermore, the performance in the determination of TC (25 μM) remained almost constant, even after CDs@SiO2-MIPs were stored at 4°C for 14 days (Figure 7C). To verify the accuracy of the sensing system, different batches of CDs@SiO2-MIPs were used to determine the TC (Figure 7D). The calculated RSD is 1.01%, indicating the high accuracy of the sensing system.

 doi:10.20944/preprints202509.0468.v1

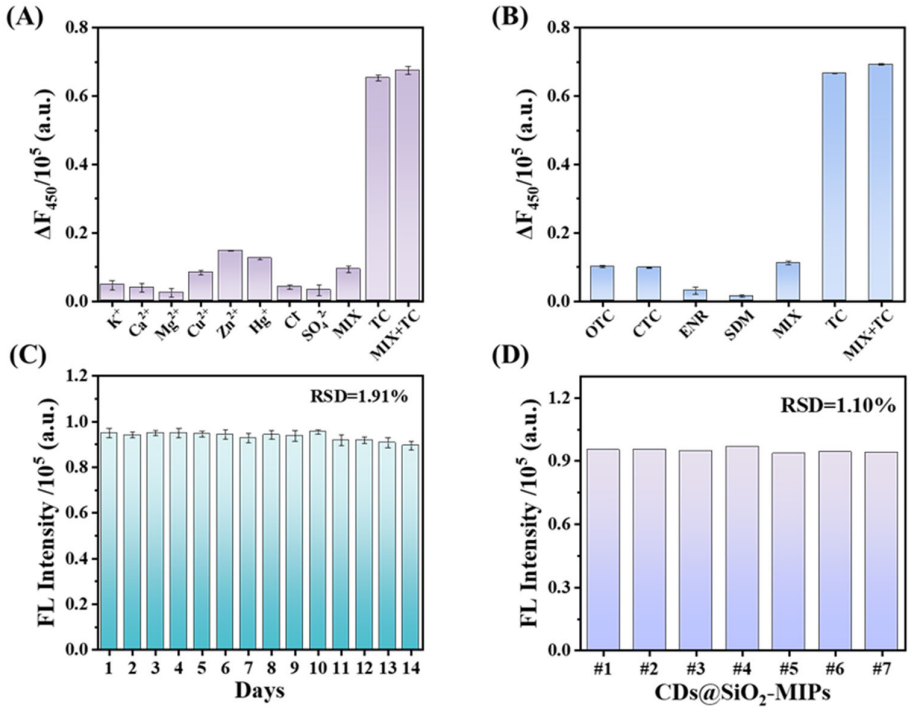

Figure 7. (A) Influence of coexisting common ions (250 μM); (B) Quenching effects of synchronous fluorescence of CDs@SiO_2-MIPs to OTC, CTC, ENR, SDM and TC in water (each of the concentrations was 250 μM; (C) The stability of the fluorescence sensing system over time; (D) The precision of sensors constructed in different batches.

3.7. Comparison with MIP-Based Sensors for TCs Detection

Compared with previously reported fluorescent sensors based on MIP, the prepared sensor has a lower detection limit and a wider linear range, making it more suitable for the detection of TCs in various matrices (Table S1). In addition, the use of harmful reagents such as volatile toxins[49,50], strong acids [51] and bases [52] that may harm health and the environment, as well as the cumbersome and complex preparation process [53,54], have been reported in literature during sensor preparation processes. The CDs@SiO_2-MIPs preparation process is simple and uses inexpensive and almost harmless raw materials, which better meets the requirements of GREENIFICATION.

4. Conclusions

In this work, a facile and effective method for the determination of TC was established based on the fluorescence quenching of the CDs@SiO_2-MIPs. Briefly, the fluorescent CDs were prepared using the hydrothermal synthesis method of tomato stalks without using any chemicals. Then, the sensor of CDs@SiO_2-MIPs was synthesized by sol-gel polymerization for enhancing the sensitivity and selectivity. The UV absorption spectra, and fluorescence lifetimes have verified that the fluorescence quenching mechanism come from IFE mechanism and static quenching. This study provides a green and simple method for the recycling and reuse of tomato stalks from facility agricultural waste. Meanwhile, the functional carbon dots derived from tomato stalks can be used as fluorescent sensing probe for the rapid and reliable investigation of environmental pollutants.

Supplementary Materials: The following supporting information can be downloaded at: https://www.mdpi.com/article/doi/s1, Figure S1: The fluorescence stability property of CDs (A) and CDs@SiO_2-MIPs (B).; Table S1: The comparison of the proposed method with other reported methods of TCs fluorescence detection.

 doi:10.20944/preprints202509.0468.v1

Author Contributions: Conceptualization, X.W. and Q.N.; Methodology, X.W. and H.D.; Validation, X.W., G.J. and J.W.; Formal Analysis, X.W., M.Z., C.T. and O.O.; Investigation, X.W., J.W., G.J., Y.Z., J.S., M.Z., X.D., Q.L., and Q.N.; Resources, X.W. and Q.N.; Data Curation, X.W. and M.Z.; Writing – Original Draft Preparation, X.W. and M.Z.; Writing – Review & Editing, X.W. and J.W. and Q.N.; Visualization, Q.N.; Supervision, H.D. and Q.N.; Project Administration, Q.N.; Funding Acquisition, H.D. and Q.N." All authors have read and agreed to the published version of the manuscript.

Acknowledgements: This work was supported by the National Natural Science Foundation of China (62101216, 32301723, 62565015), the China Postdoctoral Science Foundation (2020M671359, 2020M671367, 2022T150275), and Priority Academic Program Development of Jiangsu Higher Education Institutions (PAPD-2023-87). Postgraduate Research & Practice Innovation Program of Jiangsu Province (SJCX24_2424).

Institutional Review Board Statement: Not applicable.

Informed Consent Statement: Not applicable.

Data Availability Statement: Data are contained within the article or supplementary material. Any additional data concerning the work in this study are available on request from the corresponding author.

Conflicts of Interest: The authors declare no conflicts of interest.

References

1. Kaur, I.; Batra, V.; Kumar Reddy Bogireddy, N.; Torres Landa, S. D.; Agarwal, V., Detection of organic pollutants, food additives and antibiotics using sustainable carbon dots. *Food Chemistry* **2023,** 406, 135029.
2. Wang, M.; Xin, D.; Zhang, W.; Luo, D.; Tan, G., Defects and plasma Ag co-modified S-scheme Ag/NVs-CN/Bi_2O_2-δCO_3 heterojunction with multilevel charge transfer channels for boosting full-spectrum-driven degradation of antibiotics. *Journal of Alloys and Compounds* **2024,** 970, 172672.
3. Yang, W.; Cao, L.; Lu, H.; Huang, Y.; Yang, W.; Cai, Y.; Li, S.; Li, S.; Zhao, J.; Xu, W., Custom-printed microfluidic chips using simultaneous ratiometric fluorescence with "Green" carbon dots for detection of multiple antibiotic residues in pork and water samples. *Journal of Food Science* **2024,** 89, 5980-5992.
4. Liu, J.; Yue, Y.; Wang, W.; Tan, F.; Xia, H.; Wang, X.; Qiao, X.; Wong, P. K., Facile one-step synthesis of 3D hierarchical flower-like magnesium peroxide for efficient and fast removal of tetracycline from aqueous solution. *Journal of Hazardous Materials* **2020,** 397, 122877.
5. Yu, L.; Chen, H.; Yue, J.; Chen, X.; Sun, M.; Tan, H.; Asiri, A. M.; Alamry, K. A.; Wang, X.; Wang, S., Metal–organic framework enhances aggregation-induced fluorescence of chlortetracycline and the application for detection. *Analytical Chemistry* **2019,** 91,5913-5921.
6. Gerd Hamscher, S. S., Heinrich Höper and Heinz Nau, Determination of persistent tetracycline residues in soil fertilized with liquid manure by high-performance liquid chromatography with electrospray ionization tandem mass spectrometry. *Analytical chemistry* **2002,** 74, 1509 - 1518.
7. Zhou, Q.; Zhang, Y.; Wang, N.; Zhu, L.; Tang, H., Analysis of tetracyclines in chicken tissues and dung using LC–MS coupled with ultrasound-assisted enzymatic hydrolysis. *Food Control* **2014,** 46, 324-331.
8. Wang, Y.; Zhao, X.; Zhang, M.; Sun, X.; Bai, J.; Peng, Y.; Li, S.; Han, D.; Ren, S.; Wang, J.; Han, T.; Gao, Y.; Ning, B.; Gao, Z., Immunosorbent assay based on upconversion nanoparticles controllable assembly for simultaneous detection of three antibiotics. *Journal of Hazardous Materials* **2021,** 406, 124703.
9. Liao, S.; Liu, J.; Luo, J.; Wang, S.; Li, Y.; Li, Q.; Chen, S.; Wang, G., A ratio fluorescence probe by one-stage process for selectivity detection of tetracycline. *Optical Materials* **2022,** 134, 113160.
10. Liu, Y.; Xiao, Y.; Yu, M.; Cao, Y.; Zhang, Y.; Zhe, T.; Zhang, H.; Wang, L., Antimonene quantum dots as an emerging fluorescent nanoprobe for the pH-mediated dual-channel detection of tetracyclines. *Small* **2020,** 16,2003429.
11. Liang, N.; Hu, X.; Li, W.; Wang, Y.; Guo, Z.; Huang, X.; Li, Z.; Zhang, X.; Zhang, J.; Xiao, J.; Zou, X.; Shi, J., A dual-signal fluorescent sensor based on MoS_2 and CdTe quantum dots for tetracycline detection in milk. *Food Chemistry* **2022,** 378, 132076.
12. Guo, Y.; Cai, Z., Ascorbic acid stabilized copper nanoclusters as fluorescent probes for selective detection of tetracycline. *Chemical Physics Letters* **2020,** 759, 138048.

 doi:10.20944/preprints202509.0468.v1

13. Zou, T.; Li, S.; Yao, G.; Qu, R.; Yang, W.; Wang, H.; Tan, W.; Yang, M., Highly photoluminescent tryptophan-coated copper nanoclusters based turn-off fluorescent probe for determination of tetracyclines. *Chemosphere* **2023,** 338, 139452.
14. Li, C.; Ji, Y.; Shi, Y.; Xu, X.; Bao, L.; Cui, M.; Tian, Z.; Zhao, Z., A smart Zn-MOF-based ratiometric fluorescence sensor for accurate distinguish and optosmart sensing of different types of tetracyclines. *Applied Surface Science* **2023,** 640, 158442.
15. Liu, L.; Chen, Q.; Lv, J.; Li, Y.; Wang, K.; Li, J.-R., Stable metal–organic frameworks for fluorescent detection of tetracycline antibiotics. *Inorganic Chemistry* **2022,** 61,8015-8021.
16. Gan, Z.; Hu, X.; Xu, X.; Zhang, W.; Zou, X.; Shi, J.; Zheng, K.; Arslan, M., A portable test strip based on fluorescent europium-based metal–organic framework for rapid and visual detection of tetracycline in food samples. *Food Chemistry* **2021,** 354, 129501.
17. Shi, B.; Zhang, X.; Li, W.; Liang, N.; Hu, X.; Xiao, J.; Wang, D.; Zou, X.; Shi, J., An intrinsic dual-emitting fluorescence sensing toward tetracycline with self-calibration model based on luminescent lanthanide-functionalized metal-organic frameworks. *Food Chemistry* **2023,** 400, 133995.
18. Gao, Y.; Zhang, S.; Ge, B.; Zhao, H.; Jin, C.; Yan, H.; Zhao, L., Designing fluorescent covalent organic frameworks through regulation of link bond for selective detection of Al^{3+} and Ce^{3+}. *Spectrochimica Acta Part A: Molecular and Biomolecular Spectroscopy* **2025,** 329, 125620.
19. Yu, Y.; Jin, Q.; Ren, Y.; Wang, Y.; Zhu, D.; Wang, J., Ratiometric fluorescent sensor based on europium (III)-functionalized covalent organic framework for selective and sensitive detection of tetracycline. *Chemical Engineering Journal* **2023,** 465, 142819.
20. Gan, J.; Chen, L.; Chen, Z.; Zhang, J.; Yu, W.; Huang, C.; Wu, Y.; Zhang, K., Lignocellulosic biomass-based carbon dots: synthesis processes, properties, and applications. *Small* **2023,** 19, 2304066.
21. Yan, X.; Chen, J.-L.; Su, M.-X.; Yan, F.; Li, B.; Di, B., Phosphate-containing metabolites switch on phosphorescence of ferric ion engineered carbon dots in aqueous solution. *RSC Advances* **2014,** 4, 22318-22323.
22. Liu, Y.; Yang, H.; Huang, T.; Niu, L.; Liu, S., Recent advances of biomass-derived carbon dots with room temperature phosphorescence characteristics. *Nano Today* **2024,** 56, 102257.
23. Qi, H.; Teng, M.; Liu, M.; Liu, S.; Li, J.; Yu, H.; Teng, C.; Huang, Z.; Liu, H.; Shao, Q.; Umar, A.; Ding, T.; Gao, Q.; Guo, Z., Biomass-derived nitrogen-doped carbon quantum dots: highly selective fluorescent probe for detecting Fe^{3+} ions and tetracyclines. *Journal of Colloid and Interface Science* **2019,** 539, 332-341.
24. John, B. K.; John, N.; Korah, B. K.; Thara, C.; Abraham, T.; Mathew, B., Nitrogen-doped carbon quantum dots as a highly selective fluorescent and electrochemical sensor for tetracycline. *Journal of Photochemistry and Photobiology A: Chemistry* **2022,** 432, 114060.
25. Hu, J.; Liao, S.; Bai, Y.; Wu, S., Carbon dots derived from green jujube as chemosensor for tetracycline detection. *Journal of Environmental Chemical Engineering* **2024,** 12, 112595.
26. Sun, X.; Jiang, M.; Chen, L.; Niu, N., Construction of ratiometric fluorescence MIPs probe for selective detection of tetracycline based on passion fruit peel carbon dots and europium. *Microchimica Acta* **2021,** 188, 297.
27. Korah, B. K.; Chacko, A. R.; Mathew, S.; John, B. K.; Abraham, T.; Mathew, B., Biomass-derived carbon dots as a sensitive and selective dual detection platform for fluoroquinolones and tetracyclines. *Analytical and Bioanalytical Chemistry* **2022,** 414, 4935-4951.
28. Nie, Q.; Deng, J.; Xie, B.; Zhou, T., Highly efficient and sensitive detection of tetracycline in environmental water: Insights into the synergistic mechanism of biomass-derived carbon dots and N-methyl pyrrolidone solvent. *Talanta* **2024,** 278, 126512.
29. Zhang, Z.; Hao, R.; Li, F.; Tian, S.; Xin, X.; Li, G.; Li, D., Emulsifying properties of cellulose nanocrystals with different structures and morphologies from various solanaceous vegetable residues. *Food Chemistry* **2025,** 463, 141241.
30. Jin, K.; Ran, Y.; Alengebawy, A.; Yang, G.; Jia, S.; Ai, P., Agro-environmental sustainability of using digestate fertilizer for solanaceous and leafy vegetables cultivation: Insights on fertilizer efficiency and risk assessment. *Journal of Environmental Management* **2022,** 320, 115895.

 doi:10.20944/preprints202509.0468.v1

31. Tang, H.; Han, W.; Fei, S.; Li, Y.; Huang, J.; Dong, M.; Wang, L.; Wang, W.; Zhang, Y., Development of acid hydrolysis-based UPLC–MS/MS method for determination of alternaria toxins and its application in the occurrence assessment in solanaceous vegetables and their products. *Toxins*, **2023,** 15, 201.
32. Chen, L.; Sun, S.; Yao, B.; Peng, Y.; Gao, C.; Qin, T.; Zhou, Y.; Sun, C.; Quan, W., Effects of straw return and straw biochar on soil properties and crop growth: A review. *Frontiers in Plant Science* **2022,** 13, 986763.
33. Chen, L.; Wang, X.; Lu, W.; Wu, X.; Li, J., Molecular imprinting: perspectives and applications. *Chemical Society Reviews* **2016,** 45, 2137-2211.
34. Li, C.; Ma, Y.; Fan, C.; Kang, J.; Ma, S., A highly efficient molecularly imprinted fluorescence sensor for selective and sensitive detection of tetracycline antibiotic residues in pork. *Journal of Food Composition and Analysis* **2024,** 133, 106367.
35. Xu, Y.; Huang, T.; Wang, S.; Yan, Y., Mesoporous silica-based molecularly imprinted fluorescence sensor for the ultrafast and sensitive recognition of oxytetracycline. *Journal of Food Composition and Analysis* **2022,** 108, 104427.
36. Qiu, H.; Gao, L.; Wang, J.; Pan, J.; Yan, Y.; Zhang, X., A precise and efficient detection of Beta-Cyfluthrin via fluorescent molecularly imprinted polymers with ally fluorescein as functional monomer in agricultural products. *Food Chemistry* **2017,** 217, 620-627.
37. Mukunzi, D.; Habimana, J. d. D.; Li, Z.; Zou, X., Mycotoxins detection: view in the lens of molecularly imprinted polymer and nanoparticles. *Critical Reviews in Food Science and Nutrition* **2023,** 63, 6034-6068.
38. Arabi, M.; Ostovan, A.; Li, J.; Wang, X.; Zhang, Z.; Choo, J.; Chen, L., Molecular imprinting: green perspectives and strategies. *Advanced Materials* **2021,** 33, 2100543.
39. Ostovan, A.; Arabi, M.; Wang, Y.; Li, J.; Li, B.; Wang, X.; Chen, L., Greenificated molecularly imprinted materials for advanced applications. *Advanced Materials* **2022,** 34, 2203154.
40. Arkin, K.; Zheng, Y.; Bei, Y.; Ma, X.; Che, W.; Shang, Q., Construction of dual-channel ratio sensing platform and molecular logic gate for visual detection of oxytetracycline based on biomass carbon dots prepared from cherry tomatoes stalk. *Chemical Engineering Journal* **2023,** 464, 142552.
41. Sun, Q.; Fu, L.; Yin, C.; Wu, M.; Liu, H.; Niu, N.; Chen, L., Construction of biomass carbon dots@molecularly imprinted polymer fluorescent sensor array for accurate identification of 5-nitroimidazole antibiotics. *Sensors and Actuators B: Chemical* **2022,** 373, 132716.
42. Zhang, D.; Zhang, Y.; Li, K.; Wang, S.; Ma, Y.; Liao, Y.; Wang, F.; Liu, H., A smartphone-combined ratiometric fluorescence molecularly imprinted probe based on biomass-derived carbon dots for determination of tyramine in fermented meat products. *Food Chemistry* **2024,** 454, 139759.
43. Zhang, S.; Arkin, K.; Zheng, Y.; Ma, J.; Bei, Y.; Liu, D.; Shang, Q., Preparation of a composite material based on self-assembly of biomass carbon dots and sodium alginate hydrogel and its green, efficient and visual adsorption performance for Pb^{2+}. *Journal of Environmental Chemical Engineering* **2022,** 10, 106921.
44. Ren, Y.; Fan, Z., Synthesis of fluorescent probe based on molecularly imprinted polymers on nitrogen-doped carbon dots for determination of tobramycin in milk. *Food Chemistry* **2023,** 416, 135792.
45. Xu, L.; Fang, G.; Pan, M.; Wang, X.; Wang, S., One-pot synthesis of carbon dots-embedded molecularly imprinted polymer for specific recognition of sterigmatocystin in grains. *Biosensors and Bioelectronics* **2016,** 77, 950-956.
46. Peng, F.; Zhou, X.; Cheng, W.; Ma, J.; Jiang, H., A carbon dots probe for specific determination of cysteine based on inner filter effect. *Journal of Analytical Chemistry* **2022,** 77, 1141-1146.
47. Yuan, Y.; Jiang, J.; Liu, S.; Yang, J.; zhang, H.; Yan, J.; Hu, X., Fluorescent carbon dots for glyphosate determination based on fluorescence resonance energy transfer and logic gate operation. *Sensors and Actuators B: Chemical* **2017,** 242, 545-553.
48. Jalili, R.; Khataee, A.; Rashidi, M.-R.; Razmjou, A., Detection of penicillin G residues in milk based on dual-emission carbon dots and molecularly imprinted polymers. *Food Chemistry* **2020,** 314, 126172.
49. Li, K.; Wang, L.; Zhang, G.; Liu, J.; Du, Q., Metal-organic framework modified molecularly imprinted polymers-based sensor for fluorescent sensing of tetracycline in milk. *Journal of Molecular Structure* **2024,** 1303, 137598.

 doi:10.20944/preprints202509.0468.v1

50. Liu, C.; Song, Z.; Pan, J.; Yan, Y.; Cao, Z.; Wei, X.; Gao, L.; Wang, J.; Dai, J.; Meng, M.; Yu, P., A simple and sensitive surface molecularly imprinted polymers based fluorescence sensor for detection of λ-Cyhalothrin. *Talanta* **2014,** 125, 14-23.
51. Wang, H.; Zhao, H.; Quan, X.; Chen, S., Electrochemical determination of tetracycline using molecularly imprinted polymer modified carbon nanotube-gold nanoparticles electrode. *Electroanalysis* **2011,** 23, 1863-1869.
52. Chen, S.; Zhu, Y.; Han, J.; Zhang, T.; Chou, R.; Liu, A.; Liu, S.; Yang, Y.; Hu, K.; Zou, L., Construction of a molecularly imprinted sensor modified with tea branch biochar and its rapid detection of norfloxacin residues in animal-derived foods. *Foods*, **2023,** 12, 544.
53. Li, Y.; Li, H.; Wang, T.; Liu, G.; Wang, G.; Liu, M.; Pan, L.; He, J.; Li, K., Surface-molecularly imprinted ratiometric fluorescence sensor for fast, sensitive and selective determination of rhodamine 6G. *Dyes and Pigments* **2023,** 219, 111602.
54. Wei, X.; Hao, T.; Xu, Y.; Lu, K.; Li, H.; Yan, Y.; Zhou, Z., Facile polymerizable surfactant inspired synthesis of fluorescent molecularly imprinted composite sensor via aqueous CdTe quantum dots for highly selective detection of λ-cyhalothrin. *Sensors and Actuators B: Chemical* **2016,** 224, 315-324.